Published in final edited form as:
Biomaterials. 2011 September ; 32(27): 6412–6424. doi:10.1016/j.biomaterials.2011.05.034.

Integrin-Mediated Adhesion and Proliferation of Human MCs Elicited by A Hydroxyproline-Lacking, Collagen-like Peptide

Ohm D. Krishna[1,§], **Amit K. Jha**[1,§], **Xinqiao Jia**[1,2,*], and **Kristi L. Kiick**[1,2,*]

[1]Department of Materials Science and Engineering, University of Delaware, Newark, DE 19716, USA

[2]Delaware Biotechnology Institute, 115 Innovation Way, Newark, DE 19711, USA

Abstract

In this study, we evaluated the competence of a rationally designed collagen-like peptide (CLP-Cys) sequence - containing the minimal essential Glycine-Glutamic acid-Arginine (GER) triplet but lacking the hydroxyproline residue - for supporting human mesenchymal stem cell (hMSC) adhesion, spreading and proliferation. Cellular responses to the CLP-Cys sequence were analyzed by conjugating the peptide to two different substrates – a hard, planar glass surface and a soft hyaluronic acid (HA) particle-based hydrogel. Integrin-mediated cell spreading and adhesion were observed for hMSCs cultivated on the CLP-Cys functionalized surfaces, whereas on control surfaces lacking the peptide motif, cells either did not adhere or maintained a round morphology. On the glass surface, CLP-Cys-mediated spreading led to the formation of extended and well developed stress fibers composed of F-actin bundles and focal adhesion complexes while on the soft gel surface, less cytoskeletal reorganization was observed. The hMSCs proliferated significantly on the surfaces presenting CLP-Cys, compared to the control surfaces lacking CLP-Cys. Competitive binding assay employing soluble CLP-Cys revealed a dose-dependent inhibition of hMSC adhesion to the CLP-Cys-presenting surfaces. Blocking the $\alpha_2\beta_1$ receptor on hMSC also resulted in a reduction of cell adhesion on both types of CLP-Cys surfaces, confirming the affinity of CLP-Cys to $\alpha_2\beta_1$ receptors. These results established the competence of the hydroxyproline-free CLP-Cys for eliciting integrin-mediated cellular responses including adhesion, spreading and proliferation. Thus, CLP-Cys-modified HA hydrogels are attractive candidates as bioactive scaffolds for tissue engineering applications.

Keywords

collagen mimetic peptide; integrin; mesenchymal stem cells; hyaluronic acid; cell-adhesive surfaces

*To whom correspondence should be addressed: Xinqiao Jia, 201 DuPont Hall, Department of Materials Science and Engineering, University of Delaware, Newark, DE 19716, Phone: 302-831-6553, Fax: 302-831-4545, xjia@udel.edu, Kristi L. Kiick, 201 DuPont Hall, Department of Materials Science and Engineering, University of Delaware, Newark, DE, 19716, Phone 302-831-0201, Fax 302-831-4545. kiick@udel.edu.
§These authors contributed equally toward this work.

Introduction

Collagen proteins are abundant in extracellular matrix. In addition to their roles in imparting mechanical strength and structural integrity to various tissues such as skin, bone, cartilage, tendons and blood vessels [1], collagen contributes to the maintenance of normal cell functions. Several integrin receptor recognition sites on type I collagen have been found to be responsible for binding to multiple cells types including platelets, fibroblasts, chondrocytes and osteoblasts [1]. Such integrin-mediated collagen-cell interactions regulate the intracellular signaling pathways which play crucial roles in important biological phenomena such as platelet aggregation, cell proliferation, differentiation and apoptosis [2]. Therefore collagen scaffolds in various forms have been used for tissue engineering and wound healing applications [3]. However, full-length natural collagen extracted from animal sources has been often linked with issues like variability due to heterogeneity, difficulty in characterization, potential immunogenicity from residual animal-derived components, and risk of infection [4–7]. To circumvent these problems, the use of short collagen-like peptide (CLP) sequences containing cellular recognition domains is an attractive alternative.

Various GXX'GER hexapeptides sequences on natural collagen have been identified as integrin-binding sites. The peptide sequence GFOGER (where F is phenylalanine and O is hydroxyproline) has been identified as the crucial hexapeptide around the locus of integrin recognition on type I collagen [8–10]. Other hexapeptide sequences (such as GMOGER, GLOGER, GROGER, GASGER) have also been identified as competent for integrin recognition although with a lower affinity compared to that of GFOGER [10–12]. All of these sequences have a conserved and essential GER sequence [13]. Further more, previous studies have suggested that GEK can be substituted for GER for cell receptor binding although with somewhat lower affinity [11, 12, 14]. However, detailed studies of the cell responses (such as adhesion, spreading and proliferation) to such other sequences have not been studied for biomaterials applications. To establish the efficacy of such a short sequence as a bioadhesive support requires optimization and rigorous analyses of cell adhesion and other biological functions [2].

In many studies, CLPs have been designed mainly to mimic the conformational and higher order assembly behavior of the natural collagen [15–23]. However, these sequences do not incorporate cell binding domains to mimic the biological properties of natural collagen. To expand the use of these assembling CLPs in biological applications, Pires et. al. [24] recently reported a related collagen-like peptide that forms a fibrous three-dimensional scaffold upon metal chelation, for cell encapsulation and 3D culture purposes. In separate studies, collagen-mimetic peptides containing specific cell-binding sequence (GFOGER) have been successfully employed in various cell culture assays, and have been shown to accelerate bone regeneration in rat model [1, 25–30]. These studies collectively suggest the promise for the use of CLPs with cellular recognition domains in biomaterials applications.

We have previously reported the design of a collagen-like peptide (CLP-Cys), with the sequence $(GPP)_3GPRGEKGERGPR(GPP)_3GPCCG$, via rational choice of electrostatically stabilized amino acid triplets; this peptide exhibited a stable triple helical conformation and hierarchical assembly [31]. We designed this sequence without hydroxyproline to facilitate the potential of recombinant expression of such sequences in *E. coli*. As an additional design parameter, the CLP-Cys peptide sequence was equipped with the GEKGER sequence that was anticipated to not only electrostatically stabilize the triple helical conformation but also to impart cell and platelet adhesion [1, 31–33], which should enable structures assembled with this peptide to evoke desired cellular behavior.

In the current study, we have evaluated the cellular responses mediated through this CLP-Cys sequence; containing the minimum essential GER triplet, but lacking hydroxyproline. Glass substrates as well as hyaluronic acid (HA)-based hydrogel matrix presenting CLP-Cys peptides were chemically prepared using reductive amination chemistry. In the HA-based matrix, HA-based particles modified with the peptide (HGP-CLP-Cys), were presented as physically embedded particles in HA-based hydrogels - HA-(HGP-CLP-Cys) [34–38]. We employed human mesenchymal stem cells (hMSCs) owing to their important role in wound healing via differentiation into multiple cell types, important for both biomaterials applications and tissue engineering perspectives [39, 40].

2. Materials & Methods

2.1 Materials

Fmoc-protected amino acids, *O*-benzotriazole-*N*,*N*,*N*′,*N*′-tetramethyl-uronium-hexafluoro-phosphate (HBTU) and the rink amide 4-methylbenzhydrylamine (MBHA) resin for solid phase peptide synthesis were purchased from Novabiochem (San Diego, CA). Poly(ethylene glycol) dibutyraldehyde (Mw = 3400 Da) was purchased from Nektar Therapeutics (San Carlos, CA). Hyaluronic acid (HA, sodium salt, 500 kDa) was generously donated by Genzyme Corporation (Cambridge, MA). Piperidine, 4-methylmorpholine, dithiothreitol (DTT), adipic dihydrazide (ADH), 1-ethyl-3-[3-(dimethylamino)-propyl]carbodiimide (EDC), 1-hydroxybenzotriazole (HOBt), (N,N-dimethylamino) pyridine (DMAP), tetrabutylammonium bromide (TBAB), 2,2-dimethoxy-2-phenylacetophenone (DMPA), 1-vinyl-2-pyrrolidinone (NVP), sodium cyanoborohydride ($NaBH_3CN$), fluorescamine, glycidyl methacrylate (GMA) and 5,5′-dithiobis(2-nitrobenzoic acid (DTNB) were obtained from Aldrich (Milwaukee, WI). HPLC grade DMF (*N*-*N*-dimethyl formamide), acetonitrile, trifluoroacetic acid (TFA), acetone, hexane, ethanol, hydrochloric acid (HCl) and sodium hydroxide (NaOH) were obtained from Thermo Fisher Scientific (Waltham. MA). Bovine type I collagen was purchased from BD Bioscience (Bedford, MA), Aldehyde-functionalized glass slides were purchased from Nanocs Inc. (New York, NY). 3-(4,5-dimethythiazol-2-yl)-2,5-diphenyl tetrazolium bromide (MTT) cell proliferation assay kits were obtained from ATCC (Manassas, VA). Cascade blue hydrazide (CB, sodium salt) was purchased from Molecular Probes (Carlsbad, CA, USA). Paraformaldehyde (16% in H_2O) was obtained from Electron Microscopy Sciences (Hatfield, PA). Propidium iodide and SYTO 13 were purchased from Genway Biotech, Inc (San Diego, CA). Mouse monoclonal anti-vinculin antibody and tetramethyl rhodamine isothiocyanate (TRITC)-conjugated phalloidin were purchased from Millipore (Billerica, MA). Draq-5 was purchased from Axxora LLC (San Diego, CA). Rabbit monoclonal anti-CD44 antibody and mouse monoclonal anti-$\alpha_2\beta_1$ antibody were obtained from Abcam (Cambridge, MA). Alexa Fluor 568-labeled secondary antibody (goat anti-rabbit IgG), Alexa Fluor 488-labeled secondary antibody (goat anti-mouse IgG) were obtained from Invitrogen (Carlsbad, CA). All antibodies were diluted in 3% bovine serum albumin (BSA) in PBS (Jackson Immunoresearch, West Grove, PA).

2.2 Peptide synthesis

The CLP-Cys peptide with a sequence of $(GPP)_3GPRGEKGERGPR(GPP)_3GPCCG$ was synthesized via automated solid phase peptide synthesis procedures as described previously [31]. The crude peptide was purified via RP-HPLC and the molecular weight (3,200 Da) was confirmed via ESI-MS. The characterization data for this peptide was identical to that previously obtained [31], and the purity of the peptide was indicated to be greater than 95% via HPLC analysis. For all the subsequent reactions and experiments in this study, the CLP-Cys was first allowed to form triple helix in PBS, by incubating at 4 °C (at least overnight),

and then air oxidized at 4 °C (at least overnight) to prepare the disulfide cross-linked trimers of CLP-Cys as described earlier [31].

2.3 MTT assay

The MTT assay was conducted following the manufacturer's protocol to determine the metabolic activity of cells in the presence of the peptide at different concentrations. hMSCs were cultured at 37 °C under a 5% CO_2 humidified atmosphere in MSC growth media that contains serum (MSCGM) (Lonza Walkersville, MD). The CLP-Cys-modified glass surfaces were pre-treated with serum to ensure that substantial, non-specific protein adsorption did not occur during cell culture experiments. Confluent cells were trypsinized and seeded into 24-well plates at a density of 4×10^4 cells/well in 1 ml of culture media. The cells were allowed to attach to the wells for 4 hours. Cells cultured in the media were treated as the control and the pure media without cells was treated as the blank. Different concentrations (0.015 mg/ml to 1.5 mg/ml) of samples (with CLP-Cys in triple helical form), negative controls (with Triton X-100), and positive controls (with type I collagen) were prepared. Subsequently, the cells were cultured on the modified surfaces and controls for 3 days (without any change of media). After 3 days of culture, 100 μL of MTT reagent was added to the wells and allowed to incubate at 37 °C for an additional 4 hours. Subsequently, the cells were solubilized by adding 1 ml of sodium dodecyl sulfate (SDS) detergent and incubated overnight at room temperature (in the dark). Then, 1 ml of the solution from each well was taken and centrifuged at 4500 rpm for 5 min and 100 μl of the supernatant was placed in 96-well plates to measure the absorbance of formazan dye in the solution at 570 nm with a plate reader (Universal Microplate Analyzer). Absorbance values of each of the controls and samples were corrected by subtracting the absorbance value of the blank. The results were expressed as the normalized absorbance value with respect to the control. Five replicates of the control and all the samples at all different concentrations were analyzed.

2.4 Preparation of CLP-Cys functionalized substrates

The CLP-Cys functionalized glass slides (Glass-CLP-Cys) and HA-based hydrogels with physically embedded HGP-CLP-Cys particles [HA-(HGP-CLP-Cys)] were chemically prepared as shown in Scheme 1. The aldehyde functional groups from the Glass-CHO or the HGP-CHO were covalently conjugated to CLP-Cys peptide (presenting an N-terminal amine group) via reductive amination chemistry. First, a 3 mM CLP-Cys peptide prepared in nitrogen flushed PBS (pH 7.4, temperature 4 °C) was allowed to form triple helix for 24 hours [31]. Then the CLP-Cys peptide was air oxidized for another 24 hours at 4 °C to allow formation of disulfide bonds at the C-terminal end of the triple helix, before reaction with aldehyde. Commercially available aldehyde-functionalized glass slides (Nanocos, CGS0002) were cut into 11 mm × 11 mm pieces, and extensively washed with distilled water and then with PBS. HGP-CHO were prepared as described earlier [41]. Then, the 3 mM CLP-Cys peptide solution was allowed to react with the glass slides or the HGP-CHO particles (250 μl of 3 mM CLP-Cys peptide per mg of HGP-CHO particles) at pH 5.5 for 14 hours at 4 °C. The pH of the reaction volume was adjusted to 5.5, to ensure N-terminal site-specific reactivity as described previously [42]. Then, $NaBH_3CN$ was added (15 mM final concentration) and the reduction was allowed to proceed at room temperature for 4 hours. After 4 hours, unreacted aldehyde groups on the glass slides and the particles were passivated with glycine (3 mM) in the presence of $NaBH_3CN$ (15 mM) for another 4 hours at room temperature and subsequently extensively washed with PBS. For the glass slides, after the reaction and extensive washing with PBS, the slides were further incubated with 3 wt% BSA at 4 °C, and later extensively washed with PBS before use. Control surfaces for Glass-CLP-Cys were prepared by reacting 3 mM glycine instead of the 3 mM CLP-Cys; other reaction conditions, steps, and washing protocols were identical. This control surface

is referred as Glass-Gly in the text. For the HGP-CLP-Cys-based particles, after the reaction and extensive washing with PBS, the particles were collected via centrifugation and resuspended in PBS buffer pH 7.4 and stored at 4 °C. As a control sample for the HGP-CLP-Cys particles, HGP-Gly particles were prepared by reacting 3 mM glycine (instead of the 3 mM CLP-Cys) under the same reaction conditions, steps and washing protocol as utilized for synthesizing the HGP-CLP-Cys particles.

To construct hydrogel disks containing modified HA HGPs for the cell culture experiments, glycidyl methacrylate modified HA (HAGMA, 2 wt% in PBS, 100 μl, percent methacrylation of 11 %) was mixed with 2.5 mg of HGP-CLP-Cys or HGP-Gly. A photoinitiator solution (0.15 μL, containing 30 wt % DMPA in NVP) was then added the above suspension according to the procedure described earlier [41]. This mixture was added to a cell culture insert and then exposed to long-wavelength UV by illumination under a long-wavelength UV lamp (Model 100AP, Blak-Ray) for 20 minutes to form hydrogel disks.

2.5 Cascade blue (CB) and fluorescamine staining

For CB staining, glass slides were reacted with CB (5 mg/ml in DI water) at 37 °C in the dark for 4 h, followed by extensive wash with DI water. For fluorescamine labeling, Glass-CLP-Cys, HGP-CLP-Cys and their respective controls were suspended in PBS (pH 7.4, 100 μl), to which fluorescamine (5 mg/ml in acetone, 2 μl) was added. The reaction was allowed to proceed for 5 minutes, after which the solvent was discarded. The prepared samples after CB or fluorescamine staining were imaged with a Zeiss 5 Live Duo Laser Scanning Microscope (Carl Zeiss Inc. Thornwood, New York).

2.6 DTNB assay

To quantify the amount of CLP-Cys peptide conjugated onto the Glass-CLP-Cys or the HGP-CLP-Cys particles, the presence of free thiol groups uniquely presented via the cysteine residues present on the CLP-Cys peptide was estimated via Ellman's assay using the DTNB (5,5′-dithiobis(2-nitrobenzoic acid)) reagent [43, 44]. The cysteine residues on the CLP-Cys peptide attached on the Glass-CLP-Cys or the HGP-CLP-Cys particles were first reduced via treatment of DTT (200 mM) for 15 hours at 37 °C (every five hours DTT solution was refreshed), followed by multiple washings with excess of PBS to remove any residual DTT. Then the DTNB reagent was added and the liberated chromophore 5-mercapto-2-nitrobenzoic acid was monitored, every 10 minutes, via UV-vis at the absorption wavelength of 412 nm, until a stable absorbance value was achieved. The amount of free thiol was calculated using Beer's law and an extinction coefficient value of ε=13,600 $cm^{-1}M^{-1}$ [43, 44].

2.7 Circular dichroic (CD) spectroscopy

Characterization of the secondary structure of the CLP-Cys peptide attached on the HGP-CLP-Cys particles was conducted via circular dichroic spectroscopy (Jasco 810 circular dichroism spectropolarimeter, Jasco, Inc., Easton, MD, USA). Solutions (10 mg/ml) of the HGP-CLP-Cys (peptide pre-incubated at 4 °C for 24 hours for triple helix formation and oxidation prior to conjugation to the particles, as mentioned above) were analyzed via CD. CD spectra were recorded using quartz cells with a 0.1 cm optical path length. The spectra reported are averages of three scans. The scanning rate was 50 nm/min, with a response time of 4 s. The wavelength scans were obtained from 200 to 250 nm and were recorded every 1 nm with a 1 nm bandwidth. Data points for the thermal unfolding experiments (from 10 °C to 80 °C) were recorded at 227 nm at the heating rates of 10 °C/h with an equilibration time of 3 min.

2.8 Cell culture and cell viability

Human mesenchymal stem cells (hMSC) (Lonza, Walkersville, MD) were cultured at 37°C under a 5% CO_2 humidified atmosphere in MSC growth media (MSCGM™) (Lonza Walkersville, MD). Gel disks were synthesized as described above in the cell culture inserts. To remove any residual initiator, gel disks were incubated in PBS overnight at 37 °C. After three times washing with PBS, gel disks were soaked in 0.4 ml of serum-free media for another 4 h at 37 °C and sterilized by UV light exposure for 30 min. Confluent cells (passage 5–6) were trypsinized and the cell pellet was dispersed in the cell culture media. Cells were seeded on the top of the Glass-CLP-Cys and the gel disks, and their respective controls at the same cell density. Then, these gel disks or the Glass-CLP-Cys were incubated at 37 °C in the growth media under humidified atmosphere with 5% CO_2 and media was refreshed every three days. To assess cell viability, the cultured cells were stained with propidium iodide (1:2000 in DPBS) and SYTO 13 (1:1000 in DPBS). Images were acquired using a Zeiss 5 Live Duo Laser Scanning Microscope (Carl Zeiss Inc. Thornwood, New York).

2.9 F-actin and focal adhesion staining

Prior to labeling, gel disks or Glass-CLP-Cys and their respective controls were washed three times with PBS. Then, cells were fixed with 4% paraformaldehyde solution at room temperature for 15 min. After washing with PBS three times, cells were permeabilized by adding Triton X-100 (0.1% in PBS) at room temperature for 5 min. To avoid nonspecific binding, samples were incubated with BSA (3 wt% in PBS) at room temperature for 30 min. Then, samples were incubated with mouse anti-vinculin monoclonal primary antibody (1:200) at 4 °C for overnight. Samples were subsequently washed with PBS and incubated with Alexa Fluor 488-labeled secondary antibody (goat anti-mouse IgG, 1:100) and TRITC-labeled phalloidin (1:200) in the dark for one hour at room temperature. Prior to imaging, cell nuclei were stained with Draq-5 (1:1000) for 5 min at room temperature. After washing with PBS, confocal images were acquired using a Zeiss 5 Live Duo Laser Scanning Microscope (Carl Zeiss Inc.,Thornwood, New York).

2.10 Cell proliferation

Proliferation of hMSCs on the hydrogels disk or Glass-CLP-Cys was determined using the colorimetric alamar blue assay at 1, 7, and 14 days of culture. At a pre-determined time, the cell culture media containing 10% alamar blue was added to the samples. After 4 hr of incubation, the absorbance (550 nm) of the media aliquot (100 μl) was measured using a plate reader (Universal Microplate Analyzer). To estimate the cell number on the samples, a calibration curve was made by incubating cells in the cell culture media containing 10 % alamar blue. The cell culture media containing 10 % alamar blue was used as a blank and subtracted from the sample. Experiments were conducted in triplicate.

2.11 Assay for inhibition of cell adhesion by peptide and $\alpha_2\beta_1$ receptor blocking

Suspensions of hMSCs in serum free media were incubated with soluble peptide at different concentrations ranging from 100 nm to 20 mM and incubated for 30 minutes at 37 °C. These preincubated cells were then seeded onto the Glass-CLP-Cys slides or HA-(HGP-CLP-Cys) surface. For controls, untreated cells were seeded on the Glass-CLP-Cys slides or HA-(HGP-CLP-Cys) surface.

To estimate the number of cells on the glass slides, cells were counted with a hemocytometer. After 3 hours of incubation, the glass slides were washed with PBS. The unattached cells were collected in the PBS during the washing process. The attached cells on the glass slides were also trypsinized and collected in PBS. The attached and unattached

cells on the glass slides were counted by hemocytometry. To estimate the number of cells attached on the gel disks, an alamar blue assay was performed. First the gel disks were gently washed with PBS to remove the unattached cells and the supernatant was collected. In order to estimate the number of unattached cells, the cells collected in the supernatant were seeded on TCPS and allowed to adhere for 3 hours. The number of unattached cells in the supernatant, as well as the attached cells on the gel disks, was estimated via alamar blue assay (as described above). The percentage of adhered cells on the Glass-CLP-Cys surface or the HA-(HGP-CLP-Cys) was calculated relative to the percentage of adherent cells on the respective control surfaces. Three repeats were performed at each concentration of the peptides.

Inhibition assays for $\alpha_2\beta_1$ integrin-mediated adhesion of hMSCs were performed by blocking the $\alpha_2\beta_1$ receptors on the hMSCs. Anti-$\alpha_2\beta_1$ integrin monoclonal antibody at a concentration of 50 μg/ml was preincubated with the cells for 30 minutes at 37 °C, prior to their seeding onto the Glass-CLP-Cys plates and the HA-(HGP-CLP-Cys)[45]. For the control, untreated cells were also seeded on the Glass-CLP-Cys and HA-(HGP-CLP-Cys) surface. The percentage of adhered cells was calculated as described above. Three repeats were performed for $\alpha_2\beta_1$ blocked cells on each of the substrates.

2.12 Immunostaining of the $\alpha_2\beta_1$ integrin and CD44 receptor

For CD44 and $\alpha_2\beta_1$ integrin staining, cells were fixed and permeabilized as described above. The HA-(HGP-CLP-Cys)/cell constructs were subsequently incubated with anti-$\alpha_2\beta_1$ mouse monoclonal primary antibody (1:50) for 1 hour at room temperature. After washing with PBS, anti-CD44 rabbit monoclonal primary antibody (1:50) was added and incubated for 1 hour at room temperature. After washing with PBS, Alexa Fluor 488-labeled goat anti-mouse antibody (1:100) and Alexa Fluor 568-labeled goat anti-rabbit antibody (1:200) were added and incubated at 4 °C overnight. Prior to imaging, cell nuclei were stained with Draq-5 (1:1000) for 5 min at room temperature. After washing with PBS, confocal images were acquired using Zeiss 5 Live Duo Laser Scanning Microscope (Carl Zeiss Inc., Thornwood, New York).

2.13 Statistical analysis

All quantitative analyses were performed at least in triplicate. Results are presented as mean ± standard deviation. The significance level ($p < 0.05$) was determined by the paired students's *t*-test and is indicated in the figures.

3. Results

3.1 Cell viability in presence of soluble CLP-Cys

The potential cytotoxic effect of the chemically synthesized CLP-Cys peptide was assessed by MTT assay by culturing hMSCs in the pressence of soluble peptide at various concentrations. The peptide toxicity was compared to that monitored for natural type I collagen. The results shown in Figure 1 suggest that with respect to the control (cells seeded in pure media on TCPS), the hMSCs were viable up to 94 ± 6.2 %, 85 ± 5.3 %, and 76 ± 5.8 % at CLP-Cys peptide concentrations of 0.015, 0.15, and 1.5 mg/mL, respectively. Cell viability in the presence of the CLP-Cys peptide was found to be statistically similar ($p > 0.05$) to that observed in the presence of the native type I collagen at different concentrations.

3.2 Preparation of CLP-Cys functionalized substrates

The cellular responses to CLP-Cys peptide were monitored on both commonly employed glass surfaces as well as on HA-based materials. Surfaces presenting CLP-Cys (Glass-CLP-

Cys and HGP-CLP-Cys) were engineered by covalently conjugating the CLP-Cys to either: (i) Glass-CHO or (ii) onto 5–8 μm (diameter under isotonic conditions) HA-based hydrogel particles (HGP-CHO) [41], employing reductive amination as shown in Scheme 1. The surface density of the covalently grafted CLP-Cys peptide on the Glass-CLP-Cys and the HGP-CLP-Cys particles, calculated via the sensitive DTNB assay was 197 ± 25 picomoles/cm^2 and 1.3 ± 0.2 nanomoles/mg of HGP-CLP-Cys particles, respectively. To compare the cellular responses to the surfaces presenting CLP-Cys peptide, control surfaces were also prepared. As a control for Glass-CLP-Cys, a glycine-passivated surface was prepared (Glass-Glycine), and as a control for the HGP-CLP-Cys particles, glycine-passivated particles (HGP-Gly) were prepared. The HGP-CLP-Cys or the HGP-Gly particles were further dispersed within a HAGMA (HA-glycidyl methacrylate) precursor solution which upon UV-irradiation formed hydrogel (HA-(HGP-CLP-Cys) or the control HA-(HGP-Gly)) via photo-crosslinking of HAGMA [37].

3.3 Cascade blue and fluorescamine staining

The as-received and modified surfaces were probed with fluorescent reagents to confirm their identities; results are presented in Figure 2. The presence of the aldehyde group on the as-received Glass-CHO was probed by treatment with a cascade blue hydrazide-functionalized fluorescent probe (Figure 2a). The Glass-CHO showed positive cascade blue staining verifying the presence of the aldehyde group, while the Glass-CLP-Cys showed no fluorescence suggesting the absence of the aldehyde groups after CLP-Cys conjugation. Further, fluorescamine, a common fluorescent probe for detecting the amine groups of amino acids and proteins, was employed to confirm conjugation of CLP-Cys to the modified surfaces. Figure 2 shows positive fluorescamine labeling on the Glass-CLP and HGP-CLP surfaces. No staining was observed for the Glass-CHO surface and HGP-CHO particles prior to CLP-Cys conjugation.

3.4 Conformational behavior via CD

HGP-CLP-Cys particles (prepared via conjugation of the triple helical CLP-Cys in the oxidized form to the HGP-CHO particles) were analyzed via CD to confirm if the triple helical conformation was retained by the CLP-Cys peptide on the HGP-CLP-Cys particles. Figure 3a shows the CD wavelength spectra at different temperatures (10 °C – 80 °C) for HGP-CLP-Cys (10 mg/ml in PBS, pH 7.4), which show a positive maximum at 227 nm, consistent with the formation of triple helix. The thermal stability of the triple helical conformation of CLP-Cys on HGP-CLP-Cys was assessed by monitoring the decrease in the intensity of the mean residue ellipticity at 227 nm, as a function of increasing temperature, and was normalized to the low temperature measurement and reported as the fraction folded (Figure 3b). The melting temperature of the CLP-Cys peptide on HGP-CLP-Cys particles as deduced from the midpoint of the melting transition curve is 45 °C.

3.5 hMSC viability on CLP-Cys functionalized substrates

The viability of the hMSCs on different substrates was confirmed via live/dead staining after 3 days of culture. Data is shown in Figure 4. The staining protocol employs SYTO 13 dye to label the live cells (green) and propidium iodide to label the dead cells (red). These results show that while the majority of the hMSCs were stained in green (viable) on the Glass-CLP-Cys, HA-(HGP-CLP-Cys), and HA-(HGP-Gly) surfaces, cells were stained red (dead) on the Glass-Gly surface.

3.6 Cytoskeletal organization and focal adhesion

Adhesion-mediated cell spreading and focal adhesion was monitored after 3 hours, 3 days, and 7 days (Figure 5) via immunostaining of F-actin (red) and vinculin (green). On the

Glass-CLP-Cys surfaces at 3 hrs (Figure 5), development of stress fibers (stained in red) and vinculin (stained in green) along and at the ends of the stress fiber can be seen. Cells continued to spread with increasing culture time at day 3 and day 7 (Figure 5), as shown by the elongated and well developed stress fibers composed of actin filaments with a high degree of parallel orientation. The development of stress fibers is not observed on the Glass-Gly control substrates; there is no cell adhesion observed on these control glass surfaces (data not shown). On the HA-(HGP-CLP-Cys) (also Figure 5), minimal cell spreading was observed in 3 hours, with F-actin (stained in red) observed only around the nuclei. By day 3, the cells developed matured stress fibers. However, these stress fibers are not distinctly oriented. By day 7, cells spread considerably and displayed an interconnected filamentous intracellular network of actin with prominent stress fiber bundles. Vinculin is observed along and at the ends of the stress fibers (stained in green). On the control HA-(HGP-Gly), even by day 7, no prominent development of stress fibers is observed.

3.7 Cell proliferation

The proliferation of the hMSCs was monitored on the Glass-CLP-Cys and HA-HGP-CLP-Cys surfaces, via alamar blue assay, and is presented in Figure 6. Similar cell densities were seeded on the Glass-CLP-Cys, HA-(HGP-CLP-Cys) and HA-(HGP-Gly), and as shown in the figure, no appreciable difference in the cell density was observed on day 1 between all these samples (Figure 6). However on day 7 and day 14, a significant increase in cell density was observed for all samples. Compared to day 1, the cell density increased 2-fold and 2.5-fold on the Glass-CLP-Cys at day 7 and day 14, respectively. No proliferation of cells was observed for Glass-Gly surfaces, with values close to those of the blank at all timepoints (data not shown). Most interestingly, relative to day 1, the cell density tripled and quadrupled on HA-(HGP-CLP-Cys) at day 7 and day 14, respectively. At both the timepoints the cell density on the control HA-(HGP-Gly) was significantly lower ($p < 0.05$).

3.8 Assays for inhibition of cell adhesion by CLP-Cys and $\alpha_2\beta_1$ receptor blocking

The competitive adhesion inhibition assay is typically an indirect analysis method for identifying receptor-ligand interactions. We accordingly conducted such competitive inhibition assays for both the CLP-Cys peptide and the $\alpha_2\beta_1$ integrin; data are presented in Figure 7. Our results show that cell attachment decreases with increasing peptide concentration, illustrating a dose-dependent inhibition response for both the Glass-CLP-Cys and HA-(HGP-CLP-Cys), after pre-incubation of the cells with different concentrations of the peptide. The inhibition of cell adhesion was also analyzed by blocking cell surface receptors with an anti-integrin $\alpha_2\beta_1$ antibody with a protocol and concentration commonly reported in the literature [45]. The results (Figure 7) show that the cell binding was inhibited by 33 ± 2 % and 41 ± 5 % on Glass-CLP-Cys and HA-(HGP-CLP-Cys) respectively, by blocking the hMSC's $\alpha_2\beta_1$ receptor. In the control experiments, where mouse IgG was used for preincubation of the cells, no inhibition in cell adhesion was observed (data not shown).

3.9 Immunofluorescence staining for $\alpha_2\beta_1$ and CD44

Immunofluorescence staining for the $\alpha_2\beta_1$ integrin and the CD44 receptor on the cells attached to the HA-(HGP-CLP-Cys) gel were performed to confirm the presence of these receptors on hMSCs, and to confirm the expression of the CD44 receptor as expected for HA-mediated binding to the HA-(HGP-CLP-Cys) substrates. Figure 8 shows the positively stained images indicating the presence of both receptors, $\alpha_2\beta_1$ (green) and CD44 (red), for cells attached on the HA-(HGP-CLP-Cys) surface.

4. Discussion

The use of collagen-like peptides (CLP) in biomaterials circumvents some of the limitations associated with the use of animal-derived, full length collagen sequences such as heterogeneity, insolubility, difficulty in characterizations, and immuonogenicity [4–7]. CLP peptides employing the GFOGER sequence (identified as the $\alpha_2\beta_1$ receptor recognition site) have been shown to promote cell adhesion and spreading. The previous studies for analyzing cellular responses to GFOGER containing CLP have been performed by coating/covalent linking mainly on glass slides/TCPS. However, they have yet not been employed as a bioactive component for constructing tissue engineering constructs. Recently, Wojtowicz et. al.[28], demonstrated that a passive coating of a CLP containing GFOGER on a poly(ε-caprolactone) scaffold, even in absence of exogenous cells or growth factors, could significantly accelerate bone formation in rat femoral defect models through recruitment of osteoblasts, thus showing the promise for the use of CLPs with cellular recognition domain in biomaterials application.

We previously reported the design of a collagen-like peptide (CLP-Cys) with the sequence $(GPP)_3GPRGEKGERGPR(GPP)_3GPCCG$, that forms a thermally stable triple helix and exhibits supramolecular assembly [31]. We designed the CLP-Cys sequence by including triple helix-promoting $(GPP)_3$ triplets. The sequence was designed to be hydroxyproline-free for creating opportunities for recombinant expression of such polypeptide sequences in *E.coli*. The GPR triplet was included because it has been shown to confer stability similar to GPO in collagen triple helix host-guest peptides [46]. Furthermore GEKGER was included as electrostatically stabilizing hexapeptide and as potential cell binding sequence [1, 32, 33]. The reported peptide sequence also utilizes a type III collagen-mimetic cysteine knot at the C-terminus, known to act as a nucleating and stabilizing motif by covalently cross-linking (via air oxidation) the three peptide chains [32, 47, 48].

In this study, we have evaluated the ability of this CLP-Cys for human mesenchymal stem cell (hMSC) adhesion, spreading and proliferation. CLP-Cys was further conjugated to HA to construct a bioactive tissue engineering scaffold. HA is a biodegradable, non-antigenic, natural ECM component, recruited in wound healing [49]. The CLP-Cys peptide containing the GEKGER sequence has the potential for $\alpha_2\beta_1$ integrin-mediated binding to cells and platelets [10] and hence scaffolds constructed from CLP-Cys and HA may serve as a simplistic microenvironment in tissue engineering and wound repair.

To evaluate the cellular responses to CLP-Cys in contexts widely reported, as well as to explore the potential for a CLP-Cys/HA based tissue engineering scaffold, the CLP-Cys was covalently immobilized on two different substrates (Scheme 1) - glass as a well established flat hard substrate model and HA-(HGP-CLP-Cys) as a soft hydrogel system. The HA-based gel presents a protein-non-adhesive surface because of its hydrophilic polyanionic behavior [50, 51] and hence CLP-Cys-mediated cell adhesion and spreading could be clearly distinguished. This HA-based hydrogel system also presented a useful platform for chemical functionalization with CLP-Cys owing to its well defined chemical reactivity (facile accessibility of the reactive aldehyde functional groups) and mechanical properties (compressive modulus of ~ 20 kPa), which suggest that it may have use in applications as a tissue engineering scaffold [37, 38, 41].

Reductive amination reaction was employed for covalent conjugation of CLP-Cys to these substrates (Scheme 1); this chemistry has been successfully applied for the covalent conjugation of perlecan domain I and gelatin to HA-HGPs [38, 41]. Since the CLP-Cys peptide has a lysine residue featuring an ε-amine group (pKa = 10.5), selective reactivity of the CLP-Cys peptide via the N-terminal amine (pKa = 8.9) was ensured by maintaining the

pH of the reaction at 5.5. At this pH, the lysine amines are significantly less reactive than the N-terminal amine; site-specific N-terminal functionalization employing this approach has been demonstrated previously [42].

Prior to evaluating the detailed biological properties of the chemically synthesized CLP-Cys, the cytotoxicity of the soluble CLP-Cys peptides cultured in presence of hMSCs were determined via MTT assay, as a stringent test of cytotoxicity. These results (Figure 2) suggest that the CLP-Cys peptide in the studied concentration range did not significantly compromise the metabolic activity of hMSCs and offered cell viability similar to that of type I collagen. Although the type I collagen might be present in fibrillar form under the experimental conditions, while the CLP-Cys does not assemble, there were no apparent differences in the solubility of the collagen I and CLP-Cys. At the highest concentration of CLP-Cys studied (1.5 mg/ml) the cell viability was 76±5.8%, while at concentrations of 0.15 mg/ml, the cell viability approached 85%. In all the other cell experiments that were performed in this study, the approximate concentration of peptide, estimated from the DTNB results and mass of HA-based particles employed, was calculated to be below 0.15 mg/mL, The MTT assay results suggested the suitability of the CLP-Cys peptides in this concentration range. In subsequent studies where the peptide was immobilized on the surfaces, cell viability on the CLP-Cys modified substrates was verified through Live/Dead staining. The HA particles employed in this study are non-cytotoxic as previously shown by Jia et. al. [34].

The successful conjugation of the triple helical CLP-Cys on the Glass-CLP-Cys or the HGP-CLP-Cys substrates was qualitatively confirmed via the reaction of fluorescamine with the available amine groups from the peptide (amine from the lysine residue as well as any available unreacted N-terminal amine from the CLP-Cys trimer). Positive flourescamine labeling of CLP-Cys-functionalized surfaces (Figure 2) qualitatively confirmed the presence of the CLP-Cys on these surfaces. Quantitative estimation by DTNB assay suggested the CLP-Cys density of 197 ± 25 picomoles/cm^2 on Glass-CLP-Cys and 1.3 ± 0.2 nanomoles/mg on HGP-CLP-Cys particles.

To confirm that the triple helical structure is retained on the HGP-CLP-Cys particles after chemical conjugation, circular dichroic spectroscopy studies of the HGP-CLP-Cys particles was conducted (Figure 3). Collagens in a triple helical conformation are characterized by a weak positive ellipticity at 215–240 nm [52]; the CD spectra of HGP-CLP-Cys (Figure 3a) clearly exhibit a positive maximum at 227 nm, which decreases in intensity with increasing temperature (Figure 3b). These observations suggest that the CLP-Cys retains the triple helical conformation when attached to HGP-CLP-Cys particles, and that the triple helices retain their ability to unfold with increasing temperature. Raw ellipticity values are reported here, as no absolutely accurate estimation of peptide concentration was possible in these experiments; we present the data simply to confirm the presence of the triple helical structure and not to quantify the amount of the triple helix. It is possible that some triple helical character of the peptide is lost during the conjugation of the peptide to the particles, but sufficient triple helix remains to be detected in the CD experiments and to motivate the exploration of cell adhesion to the modified surfaces. The thermal stability of the triple helix was assessed by monitoring the CD intensity at 227 nm as a function of increasing temperature and was normalized as the fraction folded relative to the low temperature value (Figure 3b). The melting temperature of the CLP-Cys peptide on HGP-CLP-Cys particles (Figure 3b), estimated as the temperature at which the fraction folded was 0.5, is 45 °C, which is also consistent with the melting point of the unattached soluble CLP-Cys [31]. The retention, on the HGP-CLP-Cys surface, of the triple helical conformation of similar thermal stability as that in the soluble form, is consistent with expectations, as the three chains of the

CLP-Cys in triple helical form were covalently linked through disulfide bridges at the C-terminus [31] prior to their conjugation to the HA-based particles.

The hMSC viability on the various substrates was evaluated via Live/Dead staining after 3 days of culture. These results (Figure 4) indicate that although CLP-Cys functionalized surfaces (Glass-CLP-Cys and HA-(HGP-CLP-Cys) were able to support live cells (stained in green), the glycine-passivated control glass slides did not foster the attachment of live cells. These results indicate that the cell-binding ligand presented by the CLP-Cys is able to mediate cell-matrix interactions that promote cell viability. In contrast, live hMSCs in the control gel were also observed. It is possible that these cells are able to interact with the HA matrix since it is known that specific cell-surface receptors (like CD44, see Figure 8; RHAMM etc.) interact with HA [53–55].

To further analyze the CLP-Cys/hMSC interactions, cytoskeletal organization and focal adhesion studies were conducted on these substrates after 3 hours, 3 days and 7 days (Figure 5). The cells exhibited spread polygonal morphology with the development of stress fibers (stained in red) and activated vinculin (stained in green) within 3 hours on the Glass-CLP-Cys surfaces. Similar stress fiber assembly and focal adhesion associated with vinculin have been observed for different cells towards GFOGER-containing CLP sequences [26, 27]. With increasing culture time (at day 3 and 7), more elongated, oriented and well developed stress fibers composed of F-actin bundles and focal adhesion associated with vinculin along and at the end of the fibers could be observed. However, on the control Glass-Gly surfaces, very few live cells were found and the F-actin and vinculin could be seen only around the nucleus, exhibiting no spreading (data not shown). Thus, the presence of CLP-Cys on Glass-CLP-Cys surfaces can be suggested to mediate cytoskeletal reorganization and focal adhesion.

However, on the soft HA-(HGP-CLP-Cys), the development of stress fibers and focal adhesion associated vinculin were different (Figure 5). Insignificant spreading was observed in 3 hours. By day 3, noticeable F-actin filaments (stained in red) and vinculin (green) along the F-actin filaments could be observed. However, the F-actin had no regular degree of orientation and the associated vinculin was less distinct along the stress fibers. At day 7, cells spread out considerably, through elongation of stress fibers and as interconnected filamentous network. The phase contrast image (Supporting information, Figure S1 and Movie1) reveals that the cells attach to the HGP-CLP-Cys particles, and by day 3 (and more clearly by day 7), cells spread out and connect to other HGP-CLP-Cys particles. Similar spreading behaviors were observed in a previous study on this soft HA gel when gelatin was conjugated to the HGP particles [38]. In contrast, on the control HA-(HGP-Gly), cells maintained a round morphology; and the development of the stress fibers was not observed (Figure 5). F-actin was ill-defined and vinculin was localized around the nuclei even at day 7.

Taken together, the results of the cytoskeletal reorganization behavior on both the substrates indicate the role of CLP-Cys in mediating cellular adhesion and spreading, even on non-protein-adhesive HA-based surfaces. Notably, the cytoskeletal reorganization behavior of the hMSCs seeded on the hard Glass-CLP-Cys surface and soft HA-(HGP-CLP-Cys) (compressive modulus ~ 20 kPa) were not correlated in terms of chronological development of the stress fibers and their orientation, or in terms of discernable vinculin-associated focal adhesions. Cell-spreading behavior on the HA-(HGP-CLP-Cys) system can be expected to be different because it is a complicated landscape consisted of a soft gel matrix, containing HA particles of comparable size as that of cells, thus presenting a soft hydrogel system with regular surface heterogeneity. Relevant to these results, it has been previously reported that even when cells are partially embedded in a 3D matrix or placed on a soft substrate, focal

adhesions become smaller and less distinct as compared to conventional rigid substrates like glass or TCPS [56–58]. Cell spreading has also been indicated to correlate with substrate stiffness; while cells spread with well developed stress fibers and focal contact on collagen-coated hard glass surfaces, cells remained round, without signs of spreading, leading to eventual apoptosis for collagen on a soft polyacrylamide gel or pure collagen gels [59]. In contrast, in our studies on the soft HA-particle-based gels, we have observed that the cells remain viable, attach, and spread on a soft matrix displaying CLP-Cys. In addition, previous studies have also demonstrated that cell adhesion and cellular responses not only depend on receptor binding but on several other substrate-related factors such as substrate flexibility [60], substrate stiffness [59], nature of cell-substrate interface/interaction [61], height and depth of the surface irregularities presenting the cell binding ligand and the density of ligands [62–64]. In this study, we have not altered CLP-Cys density on the surfaces, which may present future opportunities for optimizing cellular responses to these materials.

Importantly, and in contrast to these previous studies [59], the hMSCs were not only viable and adhered but also continued to proliferate on the CLP-Cys presenting surfaces (Figure 6). That the CLP-Cys was an origin of the positive impact on cell proliferation in the HA-based gels is indicated by the significantly reduced proliferation of hMSCs on the control gel HA-(HGP-Gly) compared to that on the HA-(HGP-CLP-Cys). The significantly enhanced cell proliferation mediated via the presence of CLP-Cys may be advantageous for potential applications in stem cell therapy where the low number of stem cells initially available for clinical use often poses a critical limiting factor [65]. Tissue engineering constructs that can augment the viability and expansion of cells are expected to enhance tissue formation and wound healing [66–70]. Therefore, the HA-(HGP-CLP-Cys) constructs may offer important opportunities for such applications.

To more directly verify if the adhesion of hMSCs occurred through binding to the CLP-Cys and through integrin receptors, competitive adhesion inhibition assays were performed. The competitive adhesion inhibition assay is a typical indirect analysis method for identifying receptor-ligand interactions. Figure 7 shows that for both the substrates, the preincubation of hMSCs with increasing concentrations of soluble CLP-Cys reduces the number of adhered cells to these substrates. The reduction in inhibition is statistically significant between the concentrations indicated in the Figure 7 (and is not statistically significant between all the concentrations of the experiment). This dose-dependent response is more pronounced for the glass substrate. The percentage of cells attached is approximately 30% on Glass-CLP-Cys substrate, while 60% on the HA-(HGP-CLP-Cys), at 1 mM peptide concentration, indicating 70% and 40% inhibition respectively. Complete inhibition of cell adhesion could only be achieved at very high concentrations of peptide (> 5 mM). It is to be noted that the reduction in cell attachment at high peptide concentration is not attributable to any significant cell death because the total number of viable cells (sum of the cells attached and non-attached on the surfaces) as determined via alamar blue assay were statistically similar to the initial number of cells used for pre-incubation with the peptide. Therefore, the dose-dependent peptide-mediated inhibition of adhesion suggests that the peptide is able to recognize specific cell receptors and hence in its soluble form is able to block adhesion to the surfaces presenting the CLP-Cys.

Previously, it has been suggested that type I collagen-derived ligands like GFOGER and GMOEGR recognize predominantly $\alpha_2\beta_1$ receptors on the cell surface [1, 10]. The $\alpha_2\beta_1$ integrin is the only collagen-binding integrin on platelets, leading to platelet adhesion [10] and hemostasis [13], and is also involved in osteogenesis [28] as well as in the early stages of wound healing [8]. Hence $\alpha_2\beta_1$ receptor-mediated interactions can be utilized in several biomaterials applications including wound healing and tissue regeneration. Since the CLP-Cys peptide sequence was designed to contain the minimal essential GER triplet, we were

interested in determining if CLP-Cys can also recognize the $\alpha_2\beta_1$ receptor on hMSCs for integrin-mediated binding. Therefore, the inhibition of cell adhesion was analyzed by blocking the cell surface receptor with an anti-integrin $\alpha_2\beta_1$ antibody. These results presented in Figure 7, show that preincubation of hMSCs with anti- $\alpha_2\beta_1$-integrin antibody, inhibited adhesion of hMSCs by 33 ± 2 % and 41 ± 5 % on the Glass-CLP-Cys and HA-(HGP-CLP-Cys) respectively, indicating the role of $\alpha_2\beta_1$ integrin-mediated adhesion of hMSCs to the CLP-Cys. Because several integrin-recognition sites have been identified previously within collagen-derived peptide sequences [11, 14], it is thus possible that the CLP-Cys could also potentially bind to integrins other than $\alpha_2\beta_1$ on the hMSCs; a detailed study of the relative role of different integrins in binding to the CLP-Cys, however, is outside the scope of this initial study.

It is well known that CD44 is a cell-surface receptor for HA and the $\alpha_2\beta_1$ integrin is for GER-containing peptide sequences. Therefore, to acknowledge the possibility of cell-matrix interactions via both of these receptors, the hMSCs attached to the HA-(HGP-CLP-Cys) were analyzed via immunofluorescent staining for $\alpha_2\beta_1$ and CD44 (Figure 8). The positive staining for CD44 (stained in red) and $\alpha_2\beta_1$ (stained in green) can be seen along the periphery of the spread hMSCs. This corroborates the potential role of the $\alpha_2\beta_1$ integrins in cell adhesion to the CLP-Cys-modified surfaces, and also suggests the possible recruitment of CD44 receptors as may be anticipated during cell binding and spreading onto HA-based substrates. Our data thus suggest that cells are interacting with both moieties present in these hydrogel-based biomaterials.

4. Conclusion

In this study we have successfully demonstrated the biological utility of a collagen-like peptide (CLP-Cys) on functionalized glass and HA surfaces in harnessing adhesive and proliferative responses from hMSCs. The CLP-Cys compared similarly with type I collagen in being non-cytotoxic as analyzed via MTT assay. CLP-Cys could successfully be attached to the surfaces via reductive amination chemistry on aldehyde-equipped glass and HA particles, as confirmed quantitatively via DTNB assay and qualitatively via fluorescent labeling. The CLP-Cys peptide attached to the HGP-CLP-Cys particles maintained a triple helical conformation as shown via CD. The hMSCs were shown to attach to these substrates via their binding to CLP-Cys and in an $\alpha_2\beta_1$-integrin specific manner, and displayed cytoskeletal reorganization associated with development of stress fibers and focal adhesions. The CLP-Cys conjugated to HA surfaces also promoted significant proliferation of hMSCs, indicating the potential for these materials as a support matrix conducive to application in stem cell expansion and therapy. Given the role of HA in wound healing and CLPs in specific $\alpha_2\beta_1$-integrin mediated cell attachment as well as platelet aggregation, the HA/CLP-Cys matrix offers multiple useful opportunities in biomedical applications including wound healing and tissue engineering.

Supplementary Material

Refer to Web version on PubMed Central for supplementary material.

Acknowledgments

This work was funded in part by the National Science Foundation (DMR 0907478 to KLK) and the National Institutes of Health (NIH; NIH/NIDCD (1-R01-008965 to XJ)), as well as by the National Center for Research Resources (NCRR), a component of the National Institutes of Health (1-P20-RR015588 for instrument resources). Its contents are solely the responsibility of the authors and do not necessarily represent the official views of NCRR or NIH. We thank Dr. Jeffery Kaplan for his training and advice about confocal imaging, and Prof. Millicent Sullivan for advice regarding the cell culture work. We also acknowledge Genzyme for the generous gift of HA.

References

1. Reyes CD, Garcia AJ. Engineering integrin-specific surfaces with a triple-helical collagen-mimetic peptide. Journal of Biomedical Materials Research Part A. 2003; 65A:511–523. [PubMed: 12761842]
2. Garcia AJ, Reyes CD. Bio-adhesive surfaces to promote osteoblast differentiation and bone formation. Journal of Dental Research. 2005; 84:407–413. [PubMed: 15840774]
3. Glowacki J, Mizuno S. Collagen scaffolds for tissue engineering. Biopolymers. 2008; 89:338–344. [PubMed: 17941007]
4. Delustro F, Dasch J, Keefe J, Ellingsworth L. Immune-responses to allogeneic and xenogeneic implants of collagen and collagen derivatives. Clinical Orthopaedics and Related Research. 1990; 260:263–279. [PubMed: 2225633]
5. Olsen D, Yang CL, Bodo M, Chang R, Leigh S, Baez J, et al. Recombinant collagen and gelatin for drug delivery. Advanced Drug Delivery Reviews. 2003; 55:1547–1567. [PubMed: 14623401]
6. Baez J, Olsen D, Polarek JW. Recombinant microbial systems for the production of human collagen and gelatin. Applied Microbiology and Biotechnology. 2005; 69:245–252. [PubMed: 16240115]
7. Ruggiero F, Koch M. Making recombinant extracellular matrix proteins. Methods. 2008; 45:75–85. [PubMed: 18442707]
8. Emsley J, Knight CG, Farndale RW, Barnes MJ. Structure of the integrin alpha 2 beta 1-binding collagen peptide. Journal of Molecular Biology. 2004; 335:1019–1028. [PubMed: 14698296]
9. Emsley J, Knight CG, Farndale RW, Barnes MJ, Liddington RC. Structural basis of collagen recognition by integrin alpha 2 beta 1. Cell. 2000; 10:47–56. [PubMed: 10778855]
10. Farndale RW, Lisman T, Bihan D, Hamaia S, Smerling CS, Pugh N, et al. Cell-collagen interactions: the use of peptide Toolkits to investigate collagen-receptor interactions. Biochemical Society Transactions. 2008; 36:241–250. [PubMed: 18363567]
11. Raynal N, Hamaia SW, Siljander PRM, Maddox B, Peachey AR, Fernandez R, et al. Use of synthetic peptides to locate novel integrin alpha(2)beta(1)-binding motifs in human collagen III. Journal of Biological Chemistry. 2006; 281:3821–3831. [PubMed: 16326707]
12. Siljander PRM, Hamaia S, Peachey AR, Slatter DA, Smethurst PA, Ouwehand WH, et al. Integrin activation state determines selectivity for novel recognition sites in fibrillar collagens. Journal of Biological Chemistry. 2004; 279:47763–47772. [PubMed: 15345717]
13. Knight CG, Morton LF, Onley DJ, Peachey AR, Messent AJ, Smethurst PA, et al. Identification in collagen type I of an integrin alpha(2)beta(1)-binding site containing an essential GER sequence. Journal of Biological Chemistry. 1998; 273:33287–33294. [PubMed: 9837901]
14. Knight CG, Morton LF, Peachey AR, Tuckwell DS, Farndale RW, Barnes MJ. The collagen-binding A-domains of integrins alpha(1)beta(1) and alpha(2)beta(1) recognize the same specific amino acid sequence, GFOGER, in native (triple-helical) collagens. Journal of Biological Chemistry. 2000; 275:35–40. [PubMed: 10617582]
15. Przybyla DE, Chmielewski J. Higher-Order Assembly of Collagen Peptides into Nano- and Microscale Materials. Biochemistry. 2010; 49:4411–4419. [PubMed: 20415447]
16. Fields GB. Synthesis and biological applications of collagen-model triple-helical peptides. Org Biomol Chem. 2010; 8:1237–1258. [PubMed: 20204190]
17. Fallas JA, O'Leary LER, Hartgerink JD. Synthetic collagen mimics: self-assembly of homotrimers, heterotrimers and higher order structures. Chem Soc Rev. 2010; 39:3510–3527. [PubMed: 20676409]
18. Koide T. Designed triple-helical peptides as tools for collagen biochemistry and matrix engineering. Philosophical Transactions of the Royal Society B-Biological Sciences. 2007; 362:1281–1291.
19. Martin R, Waldmann L, Kaplan DL. Supramolecular assembly of collagen triblock peptides. Biopolymers. 2003; 70:435–444. [PubMed: 14648755]
20. Kotch FW, Raines RT. Self-assembly of synthetic collagen triple helices. Proceedings of the National Academy of Sciences of the United States of America. 2006; 103:3028–3033. [PubMed: 16488977]

21. Cejas MA, Kinney WA, Chen C, Leo GC, Tounge BA, Vinter JG, et al. Collagen-related peptides: Self-assembly of short, single strands into a functional biomaterial of micrometer scale. Journal of the American Chemical Society. 2007; 129:2202–2203. [PubMed: 17269769]
22. Rele S, Song YH, Apkarian RP, Qu Z, Conticello VP, Chaikof EL. D-periodic collagen-mimetic microfibers. Journal of the American Chemical Society. 2007; 129:14780–14787. [PubMed: 17985903]
23. Przybyla DE, Chmielewski J. Metal-Triggered Collagen Peptide Disk Formation. Journal of the American Chemical Society. 2010; 132:7866–7867. [PubMed: 20499839]
24. Pires MM, Przybyla DE, Chmielewski J. A Metal-Collagen Peptide Framework for Three-Dimensional Cell Culture. Angewandte Chemie-International Edition. 2009; 48:7813–7817.
25. Khew ST, Tong YW. The specific recognition of a cell binding sequence derived from type I collagen by Hep3B and L929 cells. Biomacromolecules. 2007; 8:3153–3161. [PubMed: 17854223]
26. Khew ST, Tong YW. Template-assembled triple-helical peptide molecules: Mimicry of collagen by molecular architecture and integrin-specific cell adhesion. Biochemistry. 2008; 47:585–596. [PubMed: 18154308]
27. Yamazaki CM, Kadoya Y, Hozumi K, Okano-Kosugi H, Asada S, Kitagawa K, et al. A collagen-mimetic triple helical supramolecule that evokes integrin-dependent cell responses. Biomaterials. 2010; 31:1925–1934. [PubMed: 19853297]
28. Wojtowicz AM, Shekaran A, Oest ME, Dupont KM, Templeman KL, Hutmacher DW, et al. Coating of biomaterial scaffolds with the collagen-mimetic peptide GFOGER for bone defect repair. Biomaterials. 2009; 31:2574–2582. [PubMed: 20056517]
29. Khew ST, Zhu XH, Tong YW. An integrin-specific collagen-mimetic peptide approach for optimizing Hep3B liver cell adhesion, proliferation, and cellular functions. Tissue Engineering. 2007; 13:2451–2463. [PubMed: 17596119]
30. Khew ST, Yang QJ, Tong YW. Enzymatically crosslinked collagen-mimetic dendrimers that promote integrin-targeted cell adhesion. Biomaterials. 2008; 29:3034–3045. [PubMed: 18420267]
31. Krishna OD, Kiick KL. Supramolecular Assembly of Electrostatically Stabilized, Hydroxyproline-Lacking Collagen-Mimetic Peptides. Biomacromolecules. 2009; 10:2626–2631. [PubMed: 19681603]
32. Mechling DE, Bachinger HP. The collagen-like peptide (GER)(15)GPCCG forms pH-dependent covalently linked triple helical trimers. Journal of Biological Chemistry. 2000; 275:14532–14536. [PubMed: 10799537]
33. Persikov AV, Ramshaw JAM, Kirkpatrick A, Brodsky B. Electrostatic interactions involving lysine make major contributions to collagen triple-helix stability. Biochemistry. 2005; 44:1414–1422. [PubMed: 15683226]
34. Jia XQ, Yeo Y, Clifton RJ, Jiao T, Kohane DS, Kobler JB, et al. Hyaluronic acid-based microgels and microgel networks for vocal fold regeneration. Biomacromolecules. 2006; 7:3336–3344. [PubMed: 17154461]
35. Sahiner N, Jha AK, Nguyen D, Jia XQ. Fabrication and characterization of cross-linkable hydrogel particles based on hyaluronic acid: potential application in vocal fold regeneration. Journal of Biomaterials Science-Polymer Edition. 2008; 19:223–243. [PubMed: 18237494]
36. Jha AK, Hule RA, Jiao T, Teller SS, Clifton RJ, Duncan RL, et al. Structural Analysis and Mechanical Characterization of Hyaluronic Acid-Based Doubly Cross-Linked Networks. Macromolecules. 2009; 42:537–546. [PubMed: 20046226]
37. Jha AK, Malik MS, Farach-Carson MC, Duncan RL, Jia XQ. Hierarchically structured, hyaluronic acid-based hydrogel matrices via the covalent integration of microgels into macroscopic networks. Soft Matter. 2010; 6:5045–5055. [PubMed: 20936090]
38. Jha AK, Xu X, Duncan RL, Jia X. Controlling the Adhesion and Differentiation of Mesenchymal Stem Cells Using Hyaluronic Acid-based, Doubly Crosslinked Networks. Biomaterials. 2011; 32:2466–2478. [PubMed: 21216457]
39. Sasaki M, Abe R, Fujita Y, Ando S, Inokuma D, Shimizu H. Mesenchymal stem cells are recruited into wounded skin and contribute to wound repair by transdifferentiation into multiple skin cell type. Journal of Immunology. 2008; 180:2581–2587.

40. Caplan AI. Adult mesenchymal stem cells for tissue engineering versus regenerative medicine. Journal of Cellular Physiology. 2007; 213:341–347. [PubMed: 17620285]
41. Jha AK, Yang WD, Kirn-Safran CB, Farach-Carson MC, Jia XQ. Perlecan domain I-conjugated, hyaluronic acid-based hydrogel particles for enhanced chondrogenic differentiation via BMP-2 release. Biomaterials. 2009; 30:6964–6975. [PubMed: 19775743]
42. Lee H, Jang IH, Ryu SH, Park TG. N-terminal site-specific mono-PEGylation of epidermal growth factor. Pharmaceutical Research. 2003; 20:818–825. [PubMed: 12751640]
43. Anderson WL, Wetlaufer DB. New method for disulfide analysis of peptides. Analytical Biochemistry. 1975; 67:493–502. [PubMed: 1172386]
44. Ellman GL. Tissue sulfhydryl groups. Archives of Biochemistry and Biophysics. 1959; 82:70–77. [PubMed: 13650640]
45. Feng YZ, Mrksich M. The synergy peptide PHSRN and the adhesion peptide RGD mediate cell adhesion through a common mechanism. Biochemistry. 2004; 43:15811–15821. [PubMed: 15595836]
46. Yang W, Chan VC, Kirkpatrick A, Ramshaw JAM, Brodsky B. Gly-Pro-Arg confers stability similar to Gly-Pro-Hyp in the collagen triple-helix of host-guest peptides. Journal of Biological Chemistry. 1997; 272:28837–28840. [PubMed: 9360948]
47. Barth D, Kyrieleis O, Frank S, Renner C, Moroder L. The role of cystine knots in collagen folding and stability, part II. Conformational properties of (Pro-Hyp-Gly)(n) model trimers with N- and C-terminal collagen type III cystine knots. Chemistry-a European Journal. 2003; 9:3703–3714.
48. Barth D, Musiol H, Schutt M, Fiori S, Milbradt AG, Renner C, et al. The role of cystine knots in collagen folding and stability, part I. Conformational properties of (Pro-Hyp-Gly)(5) and (Pro-(4S)-FPro-Gly)(5) model trimers with an artificial cystine knot. Chemistry-a European Journal. 2003; 9:3692–3702.
49. Garg, HG.; Hales, CA. Chemistry and biology of hyaluronan. 1st ed.. Oxford: Elsevier Ltd.; 2004.
50. Park YD, Tirelli N, Hubbell JA. Photopolymerized hyaluronic acid-based hydrogels and interpenetrating networks. Biomaterials. 2003; 24:893–900. [PubMed: 12504509]
51. Suri S, Schmidt CE. Photopatterned collagen-hyaluronic acid interpenetrating polymer network hydrogels. Acta Biomaterialia. 2009; 5:2385–2397. [PubMed: 19446050]
52. Yu YC, Berndt P, Tirrell M, Fields GB. Self-assembling amphiphiles for construction of protein molecular architecture. Journal of the American Chemical Society. 1996; 118:12515–12520.
53. Ahrens T, Sleeman JP, Schempp CM, Howells N, Hofmann M, Ponta H, et al. Soluble CD44 inhibits melanoma tumor growth by blocking cell surface CD44 binding to hyaluronic acid. Oncogene. 2001; 20:3399–3408. [PubMed: 11423990]
54. Akiyama Y, Jung S, Salhia B, Lee SP, Hubbard S, Taylor M, et al. Hyaluronate receptors mediating glioma cell migration and proliferation. Journal of Neuro-Oncology. 2001; 53:115–127. [PubMed: 11716065]
55. Murphy JF, Lennon F, Steele C, Kelleher D, Fitzgerald D, Long A. Engagement of CD44 modulates cyclooxygenase induction, VEGF generation, and cell proliferation in human vascular endothelial cells. Faseb Journal. 2005 Jan; 19(1):446–448. [PubMed: 15640281]
56. Pelham RJ, Wang YL. Cell locomotion and focal adhesions are regulated by substrate flexibility. Proceedings of the National Academy of Sciences of the United States of America. 1997; 94:13661–13665. [PubMed: 9391082]
57. Engler A, Bacakova L, Newman C, Hategan A, Griffin M, Discher D. Substrate compliance versus ligand density in cell on gel responses. Biophysical Journal. 2004; 86:617–628. [PubMed: 14695306]
58. Reinhart-King CA, Dembo M, Hammer DA. The dynamics and mechanics of endothelial cell spreading. Biophysical Journal. 2005; 89:676–689. [PubMed: 15849250]
59. Irvine DJ, Mayes AM, Griffith LG. Nanoscale clustering of RGD peptides at surfaces using comb polymers. 1. Synthesis and characterization of comb thin films. Biomacromolecules. 2001; 2:85–94. [PubMed: 11749159]
60. Banerjee P, Irvine DJ, Mayes AM, Griffith LG. Polymer latexes for cell-resistant and cell-interactive surfaces. Journal of Biomedical Materials Research. 2000; 50:331–339. [PubMed: 10737874]

61. Chollet C, Chanseau C, Remy M, Guignandon A, Bareille R, Labrugere C, et al. The effect of RGD density on osteoblast and endothelial cell behavior on RGD-grafted polyethylene terephthalate surfaces. Biomaterials. 2009; 30:711–720. [PubMed: 19010529]

62. Fraley SI, Feng YF, Krishnamurthy R, Kim DH, Celedon A, Longmore GD, et al. A distinctive role for focal adhesion proteins in three-dimensional cell motility. Nature Cell Biology. 2010; 12 598-U169.

63. Cukierman E, Pankov R, Stevens DR, Yamada KM. Taking cell-matrix adhesions to the third dimension. Science. 2001; 294:1708–1712. [PubMed: 11721053]

64. Bacakova L, Filova E, Rypacek F, Svorcik V, Stary V. Cell adhesion on artificial materials for tissue engineering. Physiological Research. 2004; 53:S35–S45. [PubMed: 15119934]

65. Rosenthal N. Youthful prospects for human stem-cell therapy - In another few decades, revised attitudes towards stem cells could lead to disease prevention and life extension. Embo Reports. 2005; 6:S30–S34. [PubMed: 15995658]

66. Drury JL, Mooney DJ. Hydrogels for tissue engineering: scaffold design variables and applications. Biomaterials. 2003; 24:4337–4351. [PubMed: 12922147]

67. Liu H, Collins SF, Suggs LJ. Three-dimensional culture for expansion and differentiation of mouse embryonic stem cells. Biomaterials. 2006; 27:6004–6014. [PubMed: 16860386]

68. Gerecht S, Burdick JA, Ferreira LS, Townsend SA, Langer R, Vunjak-Novakovic G. Hyaluronic acid hydrogen for controlled self-renewal and differentiation of human embryonic stem cells. Proceedings of the National Academy of Sciences of the United States of America. 2007; 104:11298–11303. [PubMed: 17581871]

69. Dawson E, Mapili G, Erickson K, Taqvi S, Roy K. Biomaterials for stem cell differentiation. Advanced Drug Delivery Reviews. 2008; 60:215–228. [PubMed: 17997187]

70. Prestwich GD. Engineering a clinically-useful matrix for cell therapy. Organogenesis. 2008; 4:42–47. [PubMed: 19279714]

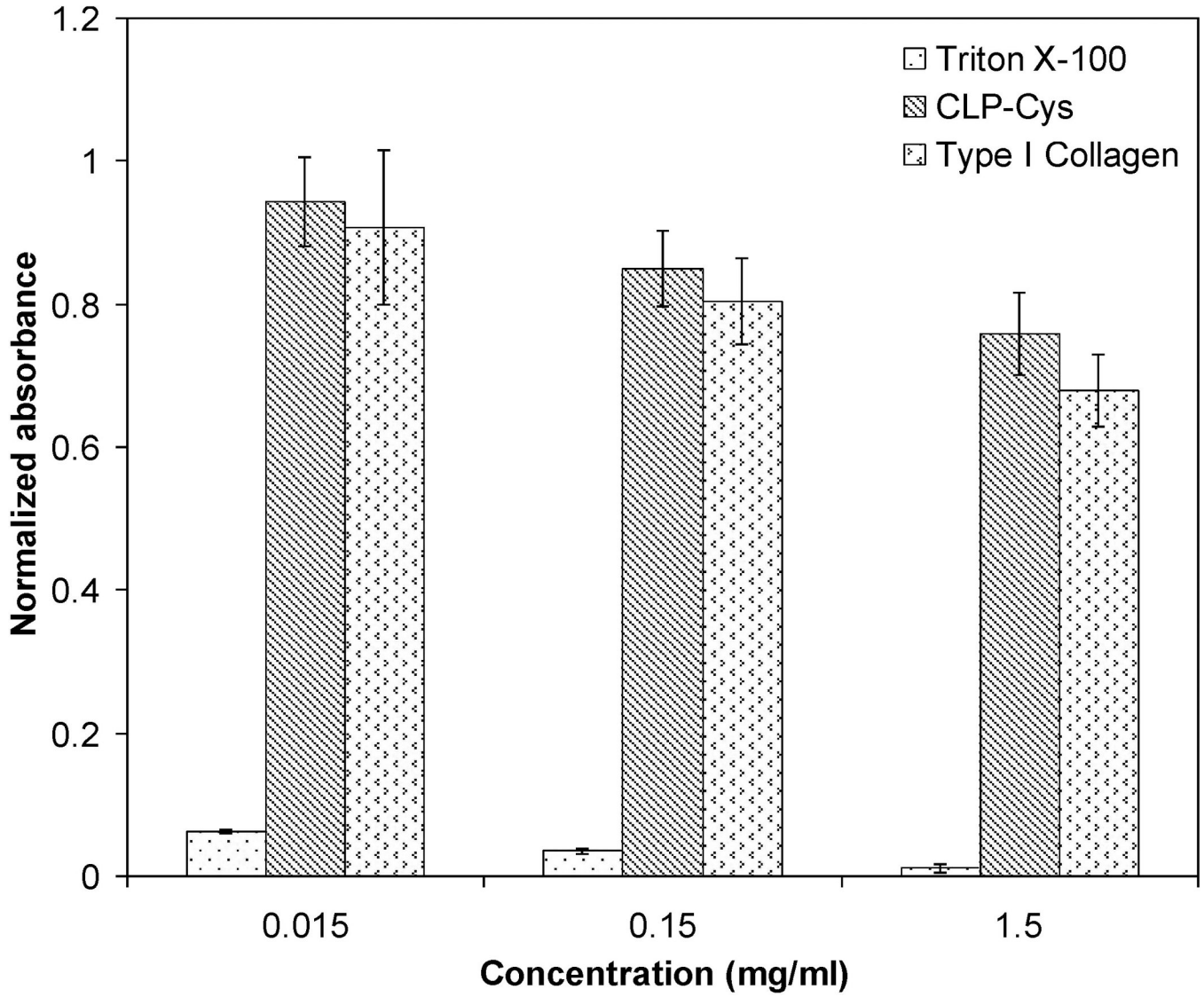

Figure 1. Cell viability assays

Normalized absorbance values indicating relative cell viability after three days of hMSC culture in the presence of CLP-Cys, Type I collagen (positive control) and Triton X-100 (negative control) at different concentrations. Data represent mean ± standard deviation of five repeats. At each concentration, the normalized absorbance value for CLP-Cys and Type I collagen were not statistically different ($p > 0.05$).

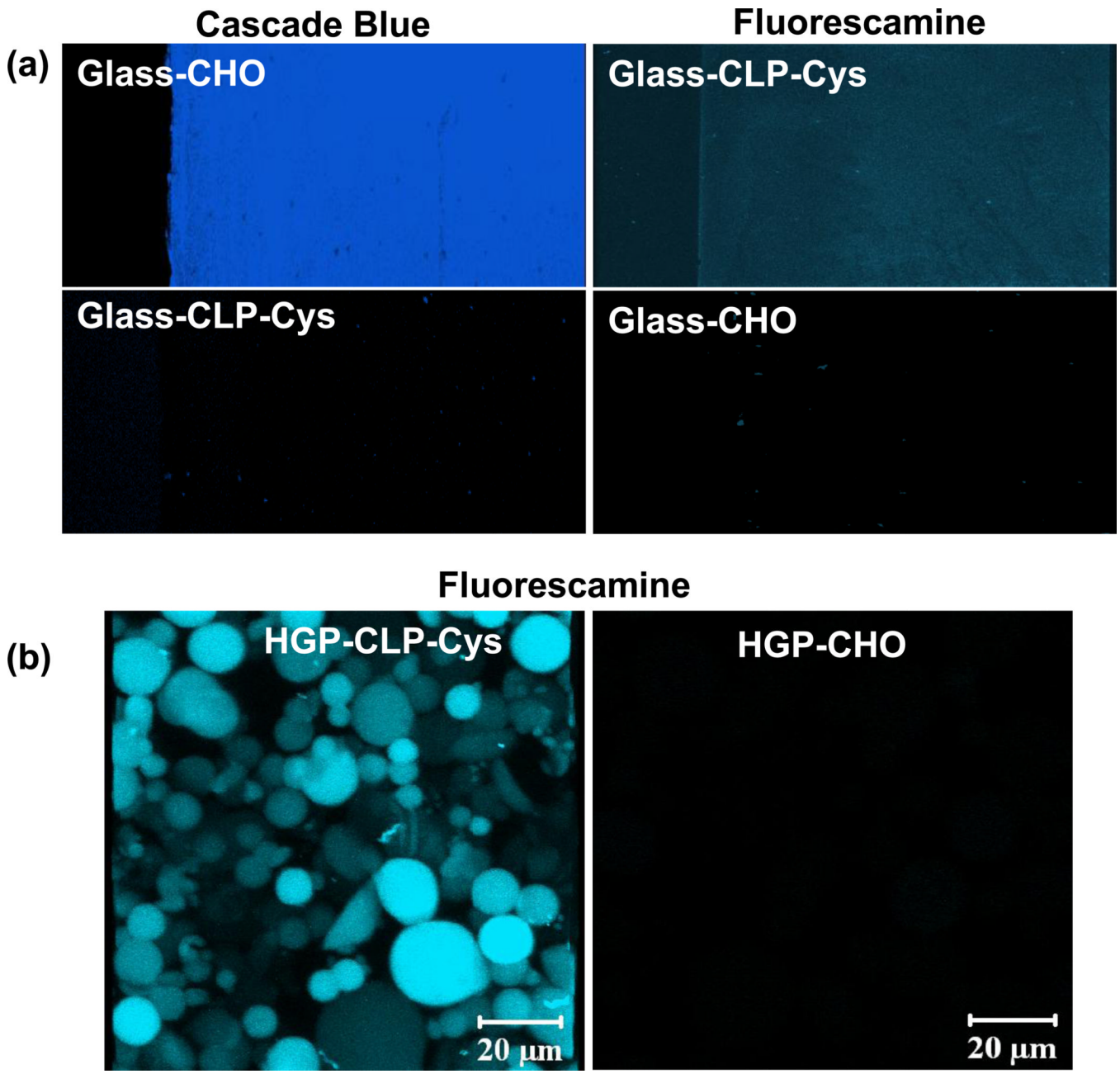

Figure 2. Surface modification results

Confocal images showing the fluorescence from (a) cascade blue hydrazide fluorescent probe on Glass-CHO and fluorescamine probe on Glass-CLP-Cys, and (b) fluorescamine probe on HGP-CLP-Cys particles. CHO-modified surfaces are clearly stained blue by treatment with cascade blue. Glass-CHO or HGP-CHO particles show no fluorescence when treated with fluorescamine due to the absence of amine groups. The Glass-CLP-Cys shows no fluorescence when treated with the cascade blue hydrazide probe suggesting the absence of aldehyde group after conjugation with CLP.

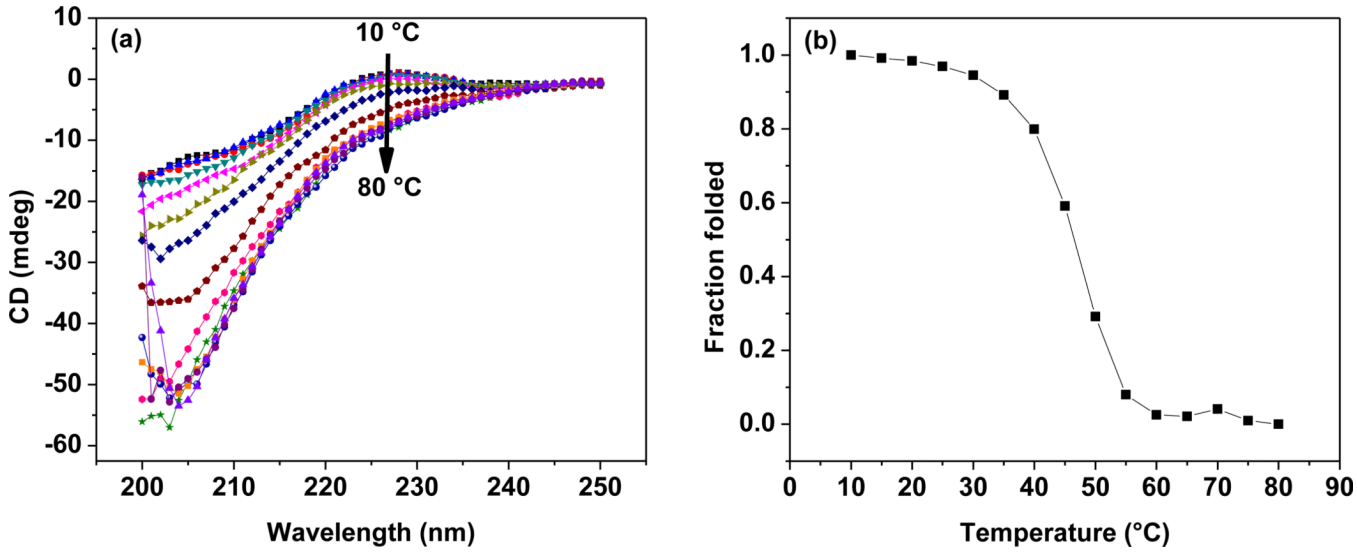

Figure 3. CD spectra of the CLP-Cys modified HA particles

Panels show (a) the full-wavelength scans for CLP-Cys covalently attached to the HGP-CLP-Cys particles (10 mg/ml in 10 mM PBS, pH 7.4), and (b) thermal transition curves. Ellipticity is presented in millidegrees owing to the lack of perfectly accurate concentration determination for these samples. In (a), the CD intensity at 227 nm at all the temperatures shows the presence of the triple helical conformation; in (b) all values were normalized to the original ellipticity values at low temperature and presented as the fraction folded.

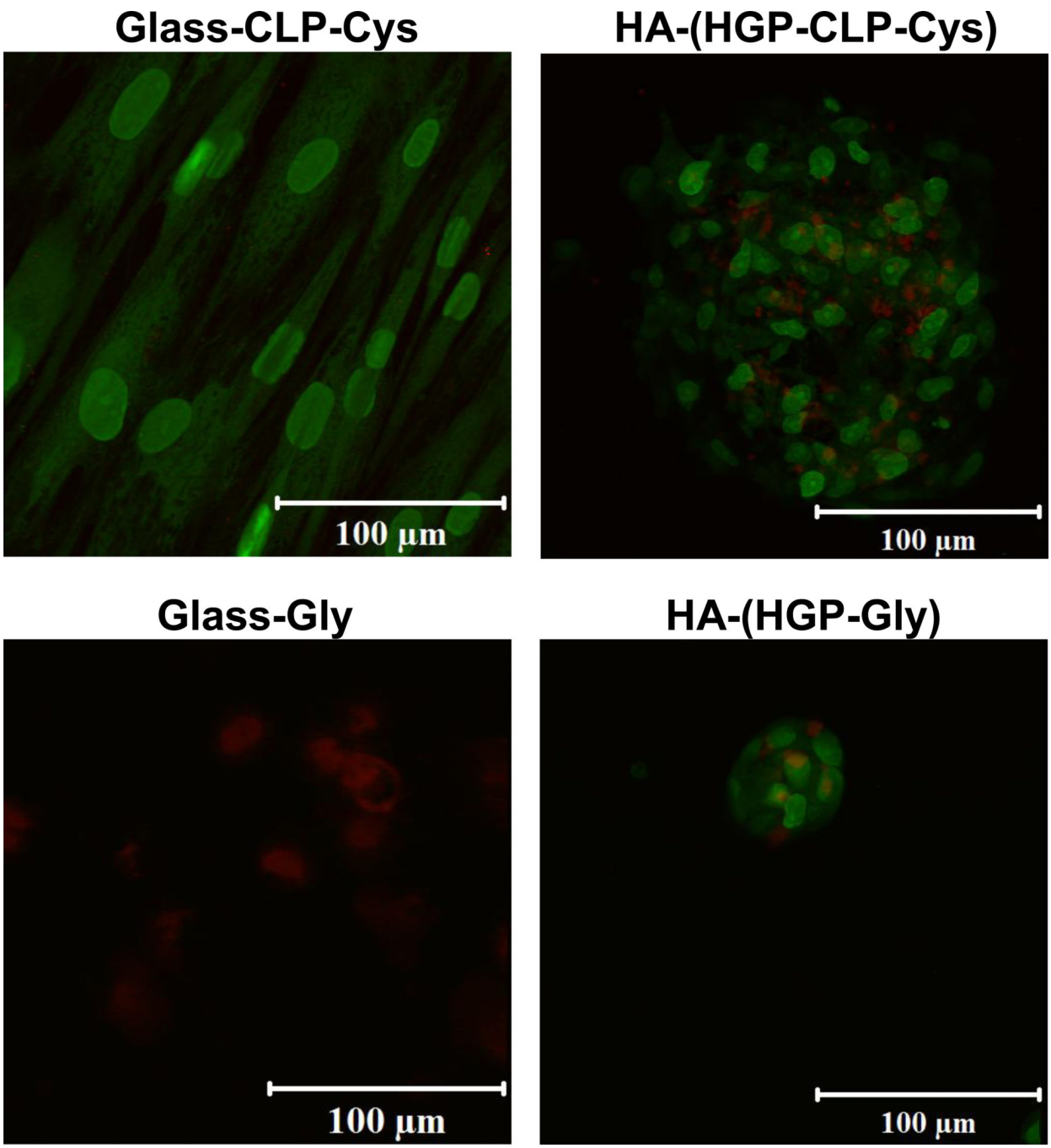

Figure 4. Live/dead staining results

Representative live/dead staining results of hMSCs cultured on Glass-CLP-Cys, Glass-Gly, HA-(HGP-CLP-Cys) and HA-(HGP-Gly) after 3 days of cell culture. Live cells are stained with Syto 13 (green) and dead cells were stained with propidium iodide (red).

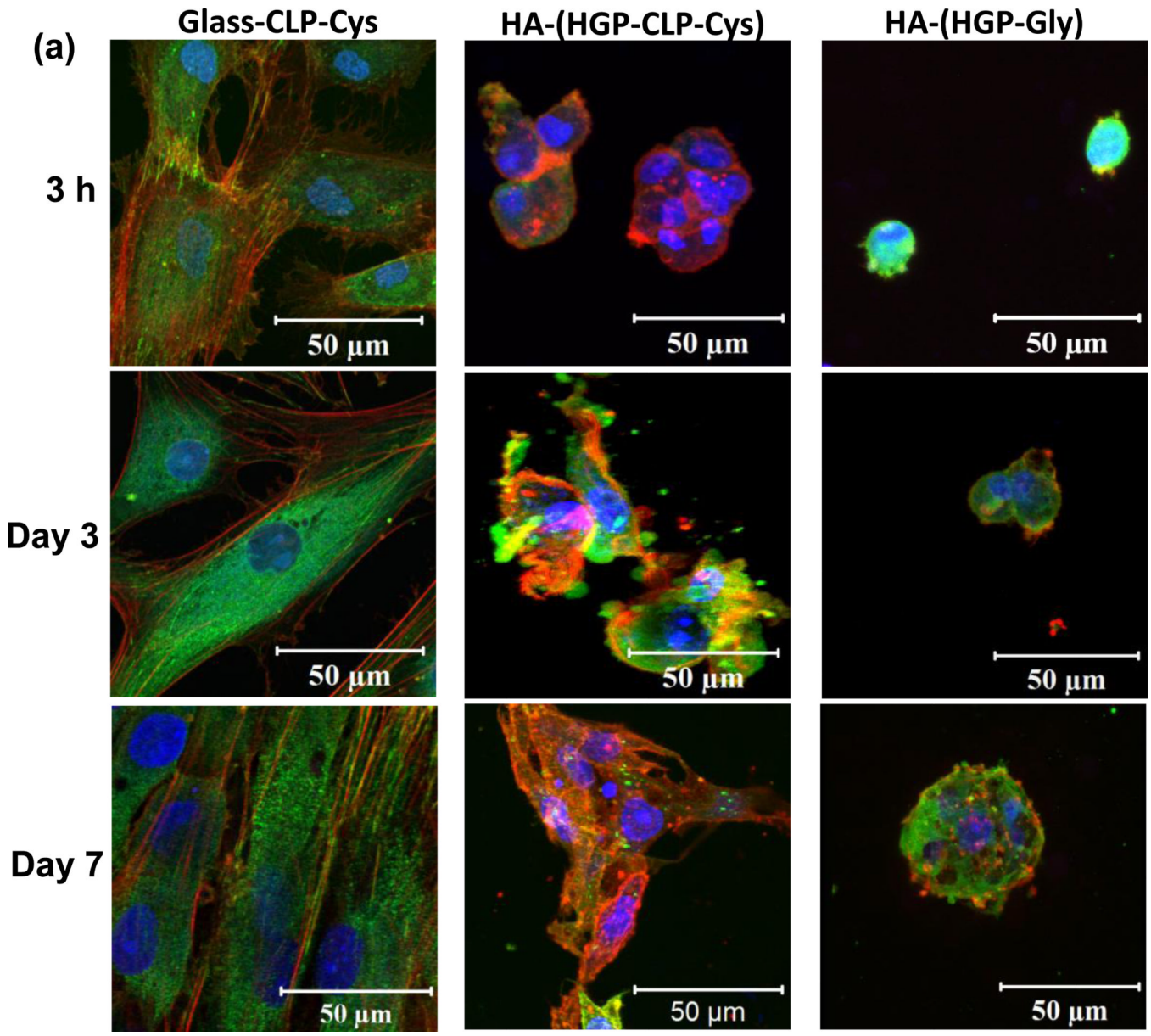

Figure 5. Immunostaining results of cell adhesion

Confocal immunofluorescence images of hMSCs adhered to the Glass-CLP-Cys, HA-(HGP-CLP-Cys) and the control HA-(HGP-Gly) arranged column-wise and horizontally at different timepoints - 3 hours, day 3, and day 7. Slices of Z-stack with the respective phase contrast images showed that hMSCs adhered on the HGP-CLP-Cys particles in the gel (Supporting information, Figure S2). Cells were fixed and stained for actin stress fibers (TRITC-phalloidin; red), nuclei (Draq5; blue) and vinculin (FITC-anti-vinculin; green).

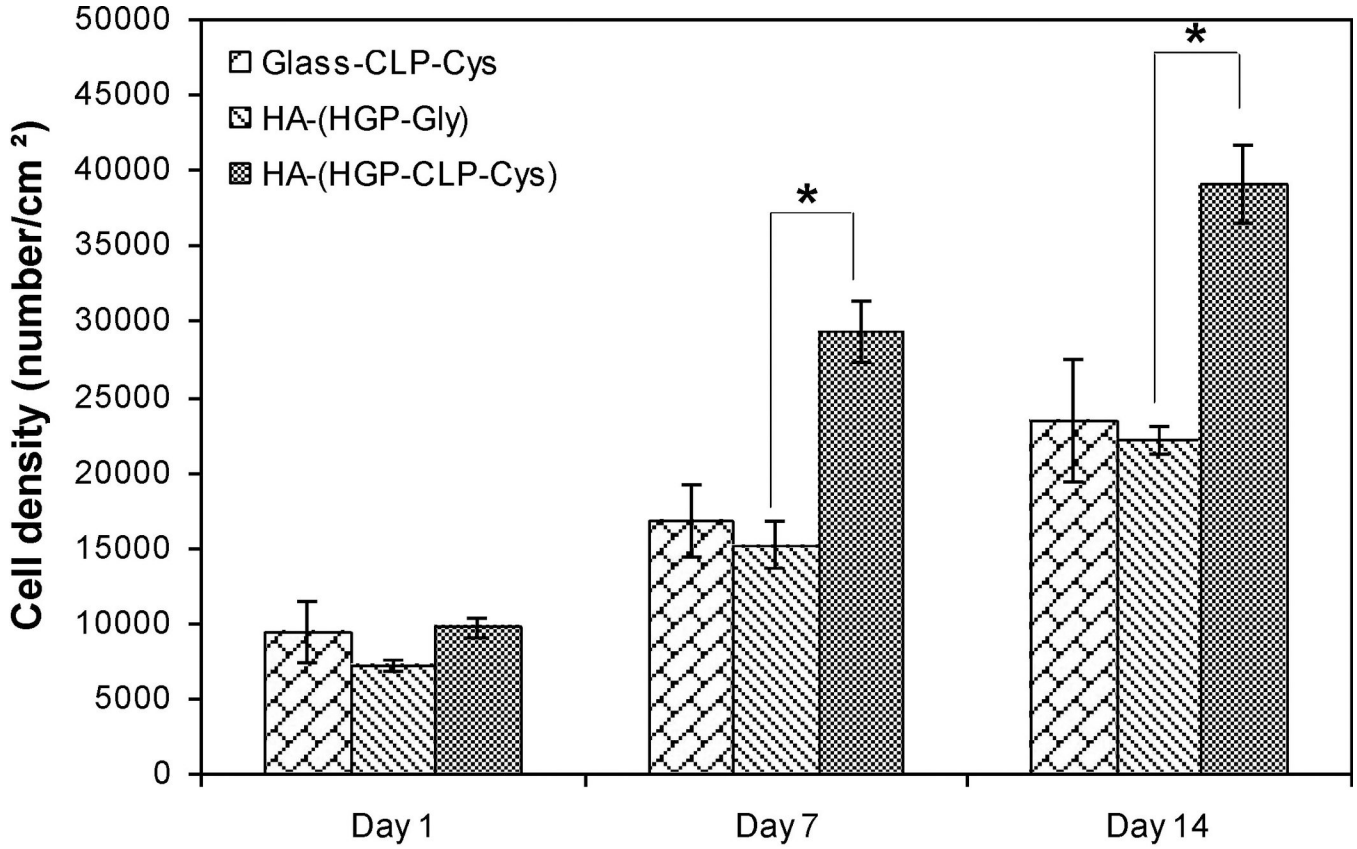

Figure 6. Cell proliferation results

Cell proliferation on Glass-CLP-Cys, HA-(HGP-Gly) and HA-(HGP-CLP-Cys). The asterisk (*) indicates data that are statistically different from each other (Student's *t* test with $p < 0.05$). Each histogram represents the mean ± standard deviation of three repeats. The Glass-Gly control did not support cell adhesion or proliferation.

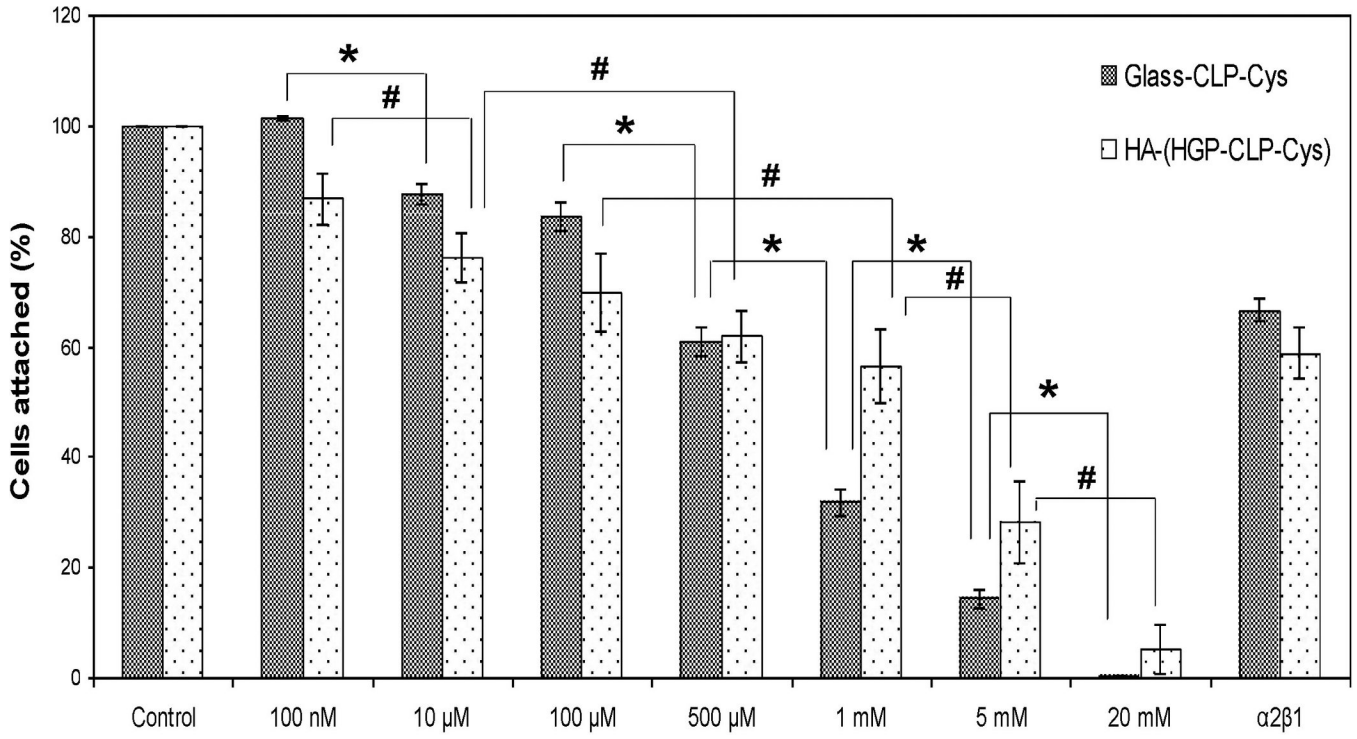

Figure 7. Inhibition of cell attachment

Inhibition of hMSCs attachment with soluble CLP-Cys peptide and anti-$\alpha_2\beta_1$ integrin antibody on Glass-CLP-Cys and HA-(HGP-CLP-Cys). Suspended cells were preincubated with different concentrations of the CLP-Cys peptide or anti-integrin $\alpha_2\beta_1$ antibody (50 μg/mL) for 30 minutes at 37 °C and then allowed to attach to the Glass-CLP-Cys or HA-(HGP-CLP-Cys). The number of hMSCs attached to these surfaces, when the hMSCs were not preincubated with either the soluble CLP-Cys or anti-$\alpha_2\beta_1$ integrin antibody was taken as 100 percent attachment. The fraction of cells attached was calculated relative to the fraction of cells that attached to the control surface. * and # are statistically different from each other (Student's *t* test with $p < 0.05$). Each histogram represents the mean ± standard deviation of three repeats.

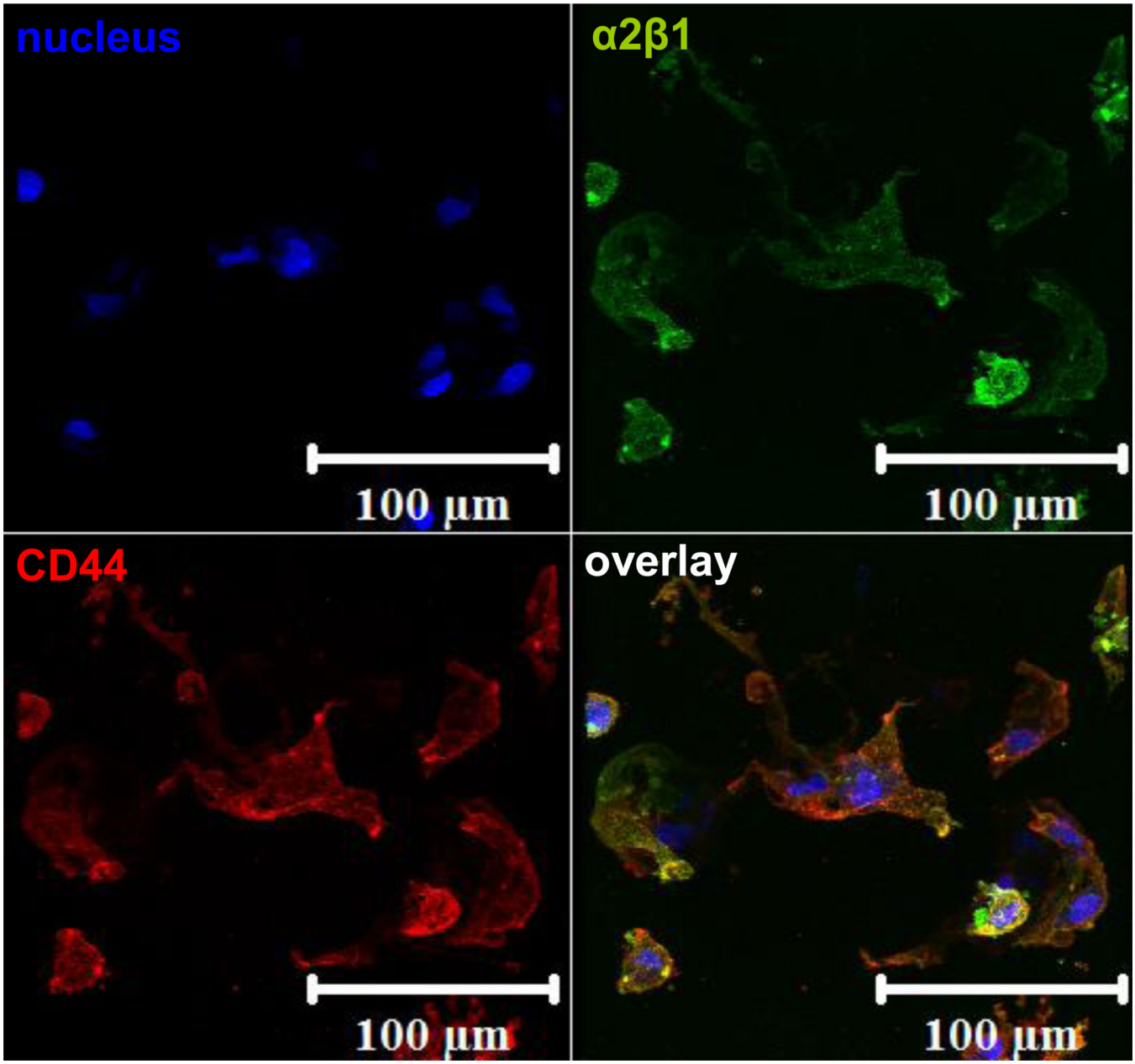

Figure 8. Staining for α2β1 and CD44

Immunofluorescent staining of $\alpha_2\beta_1$ integrin (green) and CD44 (stained red) on hMSCS attached to the HA-(HGP-CLP-Cys) after 7 days of culture. Cell nuclei were stained blue with Draq5.

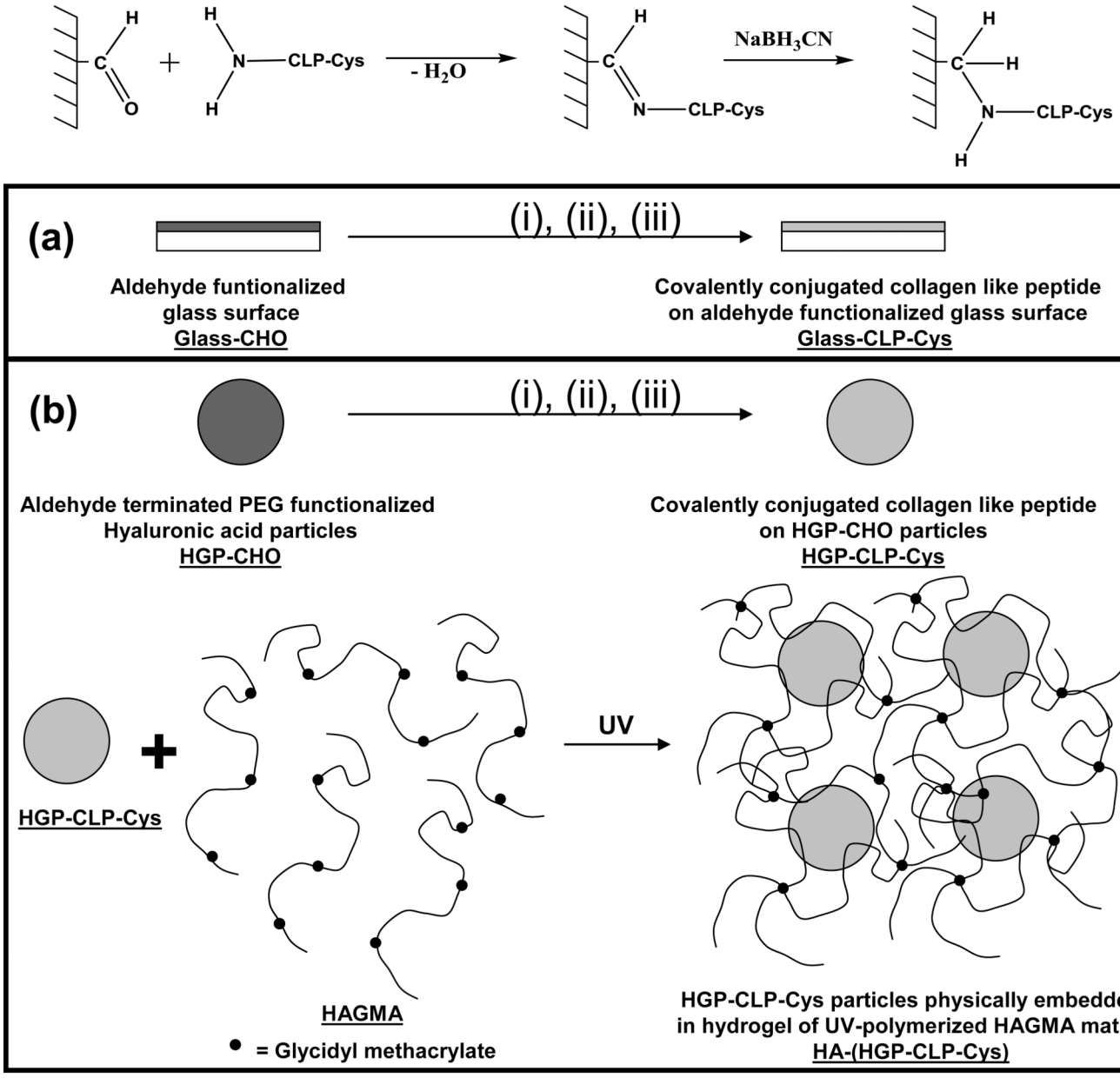

(i) 3 mM CLP-Cys in triple helical and oxidized form, PBS buffer pH =5.5, T = 4 °C, 14 hours
(ii) $NaBH_3CN$ + (i), room temperature, 4 hours
(iii) Glycine + $NaBH_3CN$, room temperature 4 hours

Scheme 1. Surface modification chemistry for generating CLP-Cys modified surfaces

Reductive amination reaction was employed for the conjugation of CLP-Cys to the aldehyde functionality on (a) aldehyde functionalized glass slides (b) HGP-CHO particles. The HGP-CLP-Cys particles were subsequently dispersed within the photo-crosslinkable HAGMA secondary matrix. UV irradiation led to the formation of the hydrogel HA-(HGP-CLP-Cys) that contains physically dispersed HGP-CLP-Cys particles.